

Cite this: *Analyst*, 2016, **141**, 5441

# An electrochemical biosensor for rapid detection of *E. coli* O157:H7 with highly efficient bi-functional glucose oxidase-polydopamine nanocomposites and Prussian blue modified screen-printed interdigitated electrodes†

Meng Xu,<sup>a</sup> Ronghui Wang<sup>a</sup> and Yanbin Li<sup>\*a,b</sup>

The presence of pathogenic bacteria in foods has always been a great threat to the wellbeing of people and the revenue of food manufacturers. Therefore, the demand for advanced detection methods that can sensitively and rapidly detect these pathogens has been of great importance. This study reports an electrochemical biosensor for rapid detection of *E. coli* O157:H7 with the integration of bifunctional glucose oxidase (GOx)–polydopamine (PDA) based polymeric nanocomposites (PMNCs) and Prussian blue (PB) modified screen-printed interdigitated microelectrodes (SP-IDMEs). The core–shell magnetic beads (MBs)–GOx@PDA PMNCs were first synthesized by the self-polymerization of dopamine (DA). Gold nanoparticles (AuNPs) were dispersed on the surface of PMNCs through biochemical synthesis to achieve further highly efficient adsorption of antibodies (ABs) and GOx. The final product ABs/GOx<sub>ext</sub>/AuNPs/MBs–GOx@PDA PMNCs served as the carrier to separate target bacteria from food matrices as well as the amplifier for electrochemical measurement. The unbound PMNCs were separated by a filtration step and transferred into glucose solution to allow the enzymatic reaction to occur. The change of the current response was measured with an electrochemical detector using PB-modified SP-IDMEs. The constructed biosensor has been proven to be able to detect *E. coli* O157:H7 with the detection limit of 10<sup>2</sup> cfu ml<sup>−1</sup>. The bifunctional PMNCs contain a high load of enzyme and can optimally utilize the binding sites on bacterial cells, which efficiently amplify the signals for measurement. The biosensor in this study exhibited good specificity, reproducibility, and stability and is expected to have a great impact on applications in the detection of foodborne pathogens.

Received 14th April 2016,  
Accepted 14th June 2016  
DOI: 10.1039/c6an00873a

www.rsc.org/analyst

## Introduction

*Escherichia coli* O157:H7 is the most common Shiga toxin-producing strain of *E. coli* in North America and can cause illness with a very low dose (10 to 100 cells). Symptoms include severe stomach cramps, bloody diarrhea, vomiting, or even life-threatening hemolytic uremic syndrome (HUS).<sup>1–3</sup> Over many decades, every outbreak related to the presence of *E. coli* O157:H7 in food products has been a serious event that caused severe problems related to human health as well as brand damage and economic loss to food manufacturers.<sup>4</sup> Most

recent cases of multistate outbreaks related to *E. coli* O157:H7 include one case associated with alfalfa sprouts that had caused nine illnesses and two hospitalizations, and the company, Jack & the Green Sprouts, Inc., had to recall all of their alfalfa and alfalfa onion sprout products.<sup>5</sup> Another case involving contaminated Costco rotisserie chicken salad had caused nineteen illnesses, five hospitalizations, and two cases of HUS.<sup>6</sup> Taylor Farms Pacific, Inc. provided the celery and onion diced blend which was suspected to be the contamination source for Costco, and had to voluntarily recall all of their products using these two ingredients. Therefore, the development of detection methods for the purpose of monitoring or screening this pathogenic bacterium in foods to prevent the catastrophic foodborne illnesses have become vitally important and caught much attention of researchers working in the area related to food safety.

There have been numerous detection methods developed over the past several decades that can detect foodborne patho-

<sup>a</sup>Department of Biological and Agricultural Engineering, University of Arkansas, Fayetteville, AR 72701, USA. E-mail: yanbinli@uark.edu; Tel: +1 (479) 575-2881

<sup>b</sup>Center of Excellence for Poultry Science, University of Arkansas, Fayetteville, AR 72701, USA

†Electronic supplementary information (ESI) available. See DOI: 10.1039/c6an00873a

gens efficiently and effectively.<sup>7–9</sup> Electrochemical biosensors, one branch that belongs to the biosensor category for rapid detection, present advantages like good sensitivity, miniaturization potential, and mass production,<sup>10</sup> and have proven to be very promising in the biosensor field. There are three common electrochemical methods: voltammetry, amperometry, and electrochemical impedance spectroscopy. Even though they are based on the measurement of the changes in different parameters, the strategies these methods employ have certain similarities.<sup>11,12</sup> These electrochemical methods employ either (1) indirect detection by forming a sandwich-like structure comprising of the target recognition element that binds to the biosensor surface and captures the target, the target bacterial cell, and the biochemical label (commonly enzyme) that triggers the reaction of the analyst in the media, or (2) direct detection by adsorbing the target bacterial cells onto the surface of the biosensor.<sup>7</sup> Both methods yield detectable changes as electric signals at the interface of the electrode and the media. With the recent advancements in nanomaterials, such as nanoporous films,<sup>13,14</sup> nanochains,<sup>15</sup> and nanotubes,<sup>16</sup> and also microfluidics<sup>14,17</sup> and screen-printed electrodes,<sup>18,19</sup> electrochemical biosensors have become more sensitive, smaller, and cheaper.

Despite all the advantages of using electrochemical biosensors for the detection of pathogenic bacteria, there are still limitations that require novel ideas to improve the performance of these sensors. Just like the two strategies mentioned previously, indirect methods require the binding of two ligands successively to the target bacteria so the detection time is prolonged, whereas when dealing with direct methods, although they have a shorter detection time due to the label-free nature, they show a relatively higher limit of detection (LOD) because they lack additional amplification.<sup>11,20–25</sup> Moreover, when using a sandwich-like mechanism which applies two ligands competing with each other for the limited binding sites and space on the surface of the bacterial cell, or using the direct adsorption of bacterial cells with spatial dimensions onto a plain surface of the electrode, it is apparent that neither of these two strategies can use the binding sites on the cell surface to the maximum potential. If there is an element that processes both functions of target recognition and electrochemical amplification, it can not only reduce the detection time, but also utilize the limited binding sites of the bacteria reaching the optimal conditions to improve the LOD.

The construction of such an element for serving dual functions as the carrier and the signal amplifier requires a good supporting matrix that can integrate individual components without losing their bioactivities as well as having a high process ability that can efficiently be modified with abundant biomolecules or nanoparticles. Since introduced by Messersmith's group,<sup>26</sup> the mussel-inspired polydopamine has gained much attention because of its excellent properties. It is well-established that, at low concentrations, initial pH values of 8 or above, and room temperature, PDA can be deposited onto various substrates as a controlled thin layer of film.<sup>27–30</sup> The rich reactive groups like catechol moieties and amines in the

PDA backbone allow PDA to bind strongly to metal ions as well as synthetic entities, like nanoparticles, polymers, or other biomolecules.<sup>27–29,31,32</sup> All of these great qualities allow PDA to be widely applied in the fabrication of nanocomposites.

Therefore, in this study, we report a novel electrochemical biosensor for the detection of *E. coli* O157:H7 based on the synthesized bifunctional polydopamine-polymeric nanocomposites that are comprised of both antibodies and glucose oxidase. For the fabrication of the electrochemical biosensor, MBs were first bound to GOx through a streptavidin–biotin reaction. After that, a thin layer of PDA film was synthesized on the MB–GOx conjugates through controlled self-polymerization of DA under alkaline conditions. The good biocompatibility of PDA allowed the GOx inside to still maintain the enzymatic activity to catalyse glucose to produce H<sub>2</sub>O<sub>2</sub> which could further reduce HAuCl<sub>4</sub> to generate AuNPs that are attached to the surface of the MBs–GOx@PDA PMNCs. With successive adsorption of ABs and additional GOx, the final product ABs/GOx<sub>ext</sub>/AuNPs/MBs–GOx@PDA PMNCs was used to capture the target bacterial cells. By using the filtration technique, the free PMNCs were filtered out and concentrated in the glucose solution for measurement. The filtration treatment helped in the isolation and concentration of the free PMNCs, meanwhile the removal of the bonded PMNCs also reduced the background noise during measurement so that the sensitivity of the developed biosensor could be correspondingly improved. The developed biosensor was also validated to detect *E. coli* O157:H7 in ground beef by using a handheld electrochemical detector. In this study, the bifunctional PMNCs have presented some valuable qualities like a short detection time due to combining the target capturing and labeling steps, effective amplification because the PMNCs contain abundant enzyme, and efficient conversion of the biological recognition to the electrochemical signal because every possible binding site on the bacteria has an active enzyme attached. This new concept has opened a new direction to construct rapid, sensitive and highly efficient electrochemical biosensors.

## Experimental

### Materials and apparatus

Phosphate buffered saline 1 (PBS1, 0.1 mol l<sup>−1</sup>, pH 7.4), dopamine (DA), gold(III) chloride hydrate, potassium ferricyanide(III), glucose, and glucose oxidase (128 200 U g<sup>−1</sup> solid) were bought from Sigma-Aldrich (St Louis, MI). Ferric chloride hexahydrate was purchased from MP Biomedicals, LLC. (Solon, OH). PBS2 (10 mmol l<sup>−1</sup>, pH 7.4) solution was prepared by diluting PBS1 at a ratio of 1 : 10, and used throughout all the tests. Ultrapure deionized water (18.2 MΩ cm) was obtained from Milli-Q (EMD Millipore, Billerica, MA). GOx was biotinylated based on the protocol reported by Kanayeva *et al.* using sulfo-NHS-biotin,<sup>33</sup> and excessive biotin was removed with a Slide-A-Lyzer dialysis kit from Pierce Protein Research Product (10 K MWCO, Rockford, IL). Streptavidin-coated magnetic



beads (MBs) with a diameter of 150 nm were manufactured by Ocean NanoTech, LLC. (San Diego, CA). Based on the information provided by the company, the superparamagnetic MBs contain 1 mg mL<sup>-1</sup> solid content (Fe) with  $2.7 \times 10^{11}$  particles per mg. The surface of MBs was covalently modified with streptavidin with a binding capacity for biotin-BSA or biotin-IgG of over 50 µg per mg or per ml. The overall structure and TEM images of the MBs were also provided by the company (Fig. S1†).

Electrochemical analysis was conducted with a CHI750B electrochemical workstation manufactured by CH Instruments (Bee Cave, TX). A BDI handheld electrochemical detector (Bio-Detection Instruments Inc., Fayetteville, AR) was used for amperometric measurement to test the food sample. The bare SP-IDME, which was designed by our group and customized by DropSens (Llanera, Spain), was constructed with six pairs of interdigitated concentric circles of gold fingers. The width of the gold fingers and the spacing between each two fingers are both 200 µm. The active area of the gold fingers is about 12.38 mm<sup>2</sup> (Fig. S2†). The MS0206 magnetic separator with a magnetic strength of approximately 1.0 Tesla (T) was purchased from Aibit LLC. (Jiangyin, China).

Rabbit anti-*E. coli* O + K polyclonal antibodies (4.0–5.0 mg mL<sup>-1</sup>) were purchased from Meridian Life Science Inc. (Memphis, TN). 1 : 5 dilutions of the antibodies (0.8–1.0 mg mL<sup>-1</sup>) were prepared with PBS and stored at 4 °C for further use, and the storage time was not more than one month. Stock bacterial cultures of *E. coli* O157:H7 (ATCC 43888), *E. coli* K12 (ATCC 29425), and *S. typhimurium* (ATCC 14028) were obtained from American Type Culture Collection (ATCC, Manassas, VA). The stock cultures were stored at –80 °C, and revived gently at room temperature when needed.

### Methods for culture preparation and media plating enumeration

The test cultures were prepared by growing the stock cultures in brain heart infusion (BHI) broth (Remel Microbiology Products, Lenexa, KS) at 37 °C for 18–20 h. A series of 1 : 10 dilutions for each bacterial culture were made with PBS2. To determine the viable cell numbers of the tested bacteria, 100 µL of each dilution were plated onto the surface of either non-selective Tryptic Soy Agar (TSA) when preparing pure laboratory culture, or selective Sorbitol MacConkey (SMAC) agar when testing the food sample. The number of bacterial colonies formed on the media after incubation at 37 °C for 18 to 24 h was counted to determine the concentration of viable

bacterial cells in terms of colony forming units per milliliter (cfu mL<sup>-1</sup>). All the cultures were prepared on the test days.

### Food sample preparation and inoculation

The detection of *E. coli* O157:H7 in ground beef (freshly purchased from a local grocery store and transported to the lab within 15 min) was examined. 25 g of ground beef was weighed and transferred into a filtering stomacher bag. After that, 225 mL of sterile PBS solution was added to the stomacher bag, and mixed using a stomacher machine (Stomacher 400, Seward, UK) at 200 rpm for two min. Nine mL of ground beef rinse water was transferred into new tubes. Then one mL of the bacterial dilution (PBS as negative control, NC) was used to spike the ground beef rinse water to achieve the desired concentration. The plate counting method was used to determine the concentration of the bacteria in ground beef rinse water. All the liquid samples right after preparation were directly used in the electrochemical analysis for the detection of *E. coli* O157:H7.

### Preparation of bifunctional PMNCs

The schematic description of the preparation of the PMNCs is shown in Fig. 1. First, 20 µL of streptavidin-coated MBs were washed with 200 µL of PBS2 to remove the preservative content in 1.5 mL low protein binding tubes (SARSTEDT AG & Co., Germany) and magnetically separated with a magnetic separator for three min. The supernatant was removed with a pipette carefully (magnetic separation procedures are the same below unless specifically mentioned). Second, the remains were mixed in 180 µL of PBS2 and 20 µL of biotin-GOx (excessive) and rotated at 15 rpm and room temperature (RT) for one hour. After the rotation finished, the yielded mixture was magnetically separated and re-dispersed into 400 µL of 0.5 mg mL<sup>-1</sup> DA (final concentration) in Tris buffer (pH 8.4, 10 mmol L<sup>-1</sup>). The mixture was rotated for another one hour to allow self-polymerization, yielding a suspension of the MBs-GOx@PDA biocomposites. After magnetic separation, the remaining biocomposites were rinsed with PBS2 three times and ultrasonically redispersed into 400 µL of PBS2. Third, the synthesis of AuNPs was based on a similar method used by Fu *et al.*<sup>34</sup> Briefly, 0.20 mmol L<sup>-1</sup> HAuCl<sub>4</sub> (in PBS2, pH 7.4) and 5 mg mL<sup>-1</sup> of glucose (both final concentration) were successively mixed in the yielded suspension for 5 h at 4 °C to allow biochemical synthesis of AuNPs on the surface of the MBs-GOx@PDA biocomposites. The dispersion of AuNPs on the surface of MBs-GOx@PDA PMNCs could help with adsorption of ABs and GOx more efficiently.<sup>34</sup> Finally, the synthesized AuNPs/MBs-



Fig. 1 The schematic illustration of the ABs/GOx<sub>ext</sub>/AuNPs/MBs-GOx@PDA PMNCs synthesis.



GOx@PDA biocomposites were suspended into the solution containing excessive anti-*E. coli* polyclonal ABs overnight at 4 °C. After magnetic separation, the ABs/AuNPs/MBs-GOx@PDA PMNCs were mixed with 5 mg ml<sup>-1</sup> GOx for 1 h at room temperature to block the unspecific attachment and to allow an additional load of enzyme on the PMNCs. The prepared ABs/GOx<sub>ext</sub>/AuNPs/MBs-GOx@PDA PMNCs were stored at 4 °C when not in use.

### Preparation of a Prussian blue modified SP-IDME

The bare SP-IDME was first thoroughly cleaned based on the reported protocol.<sup>35</sup> The surface of the SP-IDME was carefully polished in alumina slurry with 0.02–0.05 μm particles. After rinsing with Milli-Q water thoroughly, the electrodes were ultrasonically treated for 2 min to remove the residual alumina particles. After that, the electrodes were rinsed with Milli-Q water again and dried in the oven at 80 °C for 1 h.

The electrochemical deposition of Prussian blue on the surface of the SP-IDME was performed by using cyclic voltammetry (CV) based on the procedure described by Lin *et al.* with minor changes.<sup>36</sup> First, the bare SP-IDME was voltammetrically pre-treated from -1.7 V to 1.7 V for 1 cycle. Second, 50 μl of aqueous solution containing 50 mmol l<sup>-1</sup> of FeCl<sub>3</sub>, K<sub>4</sub>Fe(CN)<sub>6</sub>, 0.1 mol l<sup>-1</sup> KCl, and 0.01 mol l<sup>-1</sup> HCl (all final concentration) were dropped to cover the entire active surface of the SP-IDME. The deposition of the PB was accomplished by applying -0.5 V to 0.5 V at a rate of 0.05 V s<sup>-1</sup> for 2 cycles. The excessive solution was carefully washed off by Milli-Q water and the electrode was dried with nitrogen gas. Finally, 50 μl of aqueous solution containing 0.1 mol l<sup>-1</sup> KCl and 0.01 mol l<sup>-1</sup> HCl was dropped onto the surface of the SP-IDME. The electrode was electrochemically cycled from -0.5 V to 0.5 V at a rate of

0.1 V s<sup>-1</sup> for 15 cycles until a stable CV curve was obtained. When not in use, the modified SP-IDMEs were kept in the desiccator at room temperature.

### Construction of the electrochemical biosensor for the detection of *E. coli* O157:H7

As illustrated in Fig. 2, the construction and mechanism of the electrochemical biosensor are described as follows. First, after blocking with GOx, the ABs/GOx<sub>ext</sub>/AuNPs/MBs-GOx@PDA PMNCs were thoroughly washed with PBS2 three times and ultrasonically dispersed in PBS2 each time. The final ABs/GOx<sub>ext</sub>/AuNPs/MBs-GOx@PDA PMNCs were mixed with 200 μl of *E. coli* O157:H7 dilutions with a controlled concentration for 45 min at room temperature to allow the capture of the target bacteria. Third, the PMNCs-cell conjugates were magnetically separated, washed with PBS2 three times, and suspended in 200 μl of PBS2. Then, the suspension was filtered through a filter paper (EMD Millipore) with a pore size of 0.8 μm using a syringe (BD Syringes, Franklin Lakes, NJ) and a filter holder (EMD Millipore) into a new tube (1.5 ml). 600 μl of PBS2 were used to wash the free PMNCs thoroughly off the filter paper. Finally, the solution containing filtered-out free PMNCs was magnetically separated for 5 min. Then 50 μl of 10 mmol l<sup>-1</sup> glucose solution (in PBS2) were added to allow enzymatic reaction for 5 min. 50 μl of sample were dropped onto the PB-modified SP-IDME for electrochemical analysis. Both CV and amperometric detection were used to characterize and detect different concentrations of target bacteria.

The specificity of the constructed biosensor was investigated by testing other non-target bacteria, such as *E. coli* K12 and *S. typhimurium*. The concentration of the target and the non-target bacteria tested was 10<sup>4</sup> cfu ml<sup>-1</sup>. The BDI handheld

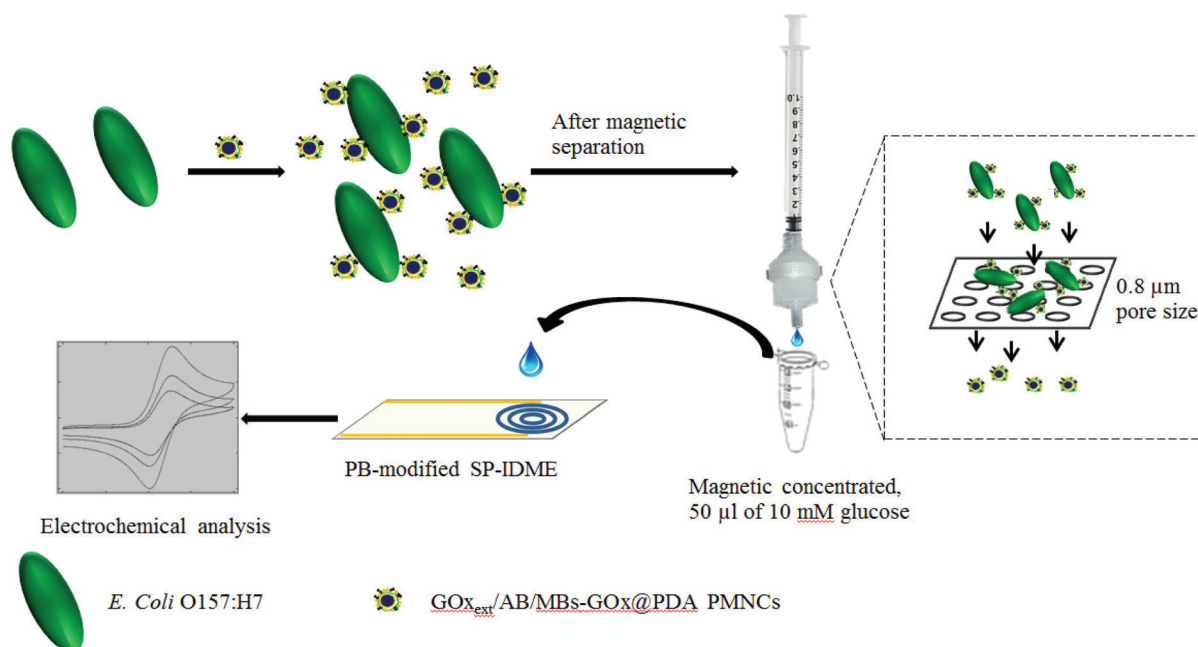


Fig. 2 The construction of the electrochemical biosensor for the detection of *E. coli* O157:H7.



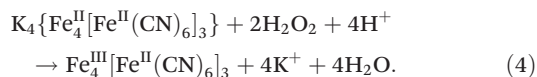
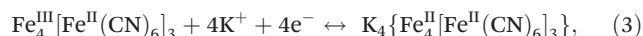
electrochemical detector was used to validate the concept for the detection of the target bacteria in the concentration range of  $10^1$  to  $10^5$  cfu  $\text{ml}^{-1}$  in ground beef.

The statistical analysis of data, such as the mean, standard deviation, and linear regression relationship, was performed using Excel 2010 software (Microsoft, Redmond, WA) with at least three replications for experiments.

## Results and discussion

### Characterization of the PB-modified SP-IDME

Since the concept of glucose biosensors was first introduced in 1962,<sup>37</sup> there have been numerous electrochemical methods developed to monitor the concentration of glucose in solution.<sup>38–41</sup> Currently, most commercial glucose biosensors do not operate very differently from the concept of the second-generation glucose biosensors which use soluble or immobilized mediators to help with the charge transfer between the enzyme and the electrode.<sup>41</sup> Prussian blue, a mixture of ferric and ferrous cyanide, is one of the most common mediators. The mechanism of using PB to detect glucose is based on the following reactions (GOx as the catalytic enzyme).<sup>42,43</sup>



Even now, PB mediated electrochemical biosensors are still under intensive study to construct sensitive, cheap, and reproducible electrodes or strips to monitor the concentration of glucose in different media.

Therefore, PB was used as the mediator to modify the SP-IDME for the purpose of constructing a cheap and easily reproducible measurement method to monitor the enzymatic reaction of glucose in this study. In order to evaluate the performance of the constructed biosensor, the characteristics of the PB-modified SP-IDME must be clarified first (Fig. 3). During the electrodeposition of PB onto the surface of the SP-IDME (Fig. 3(a)), the CV curve of cycle 1 was different from those of cycles 2 and 3, indicating the formation of a PB film onto the electrode. The CV curves of cycles 2 and 3 show almost the same shape, indicating that there is no significant change of the PB film deposited onto the electrode surface after cycle 2, which was determined to be used as the duration of PB electrodeposition for the following electrode modification. Fig. 3(b) to (d) show the performance of the PB-modified SP-IDME when used for the electrochemical measurement of  $\text{H}_2\text{O}_2$  at different concentrations. When  $\text{H}_2\text{O}_2$  was present in the solution, one redox peak was shown at  $-0.8$  V, and a higher concentration of  $\text{H}_2\text{O}_2$  caused a higher current response (Fig. 3(b)). The presence of  $1 \text{ mol l}^{-1}$  and  $0.1 \text{ mol l}^{-1}$   $\text{H}_2\text{O}_2$  gave an exceedingly large current response, and also damaged the

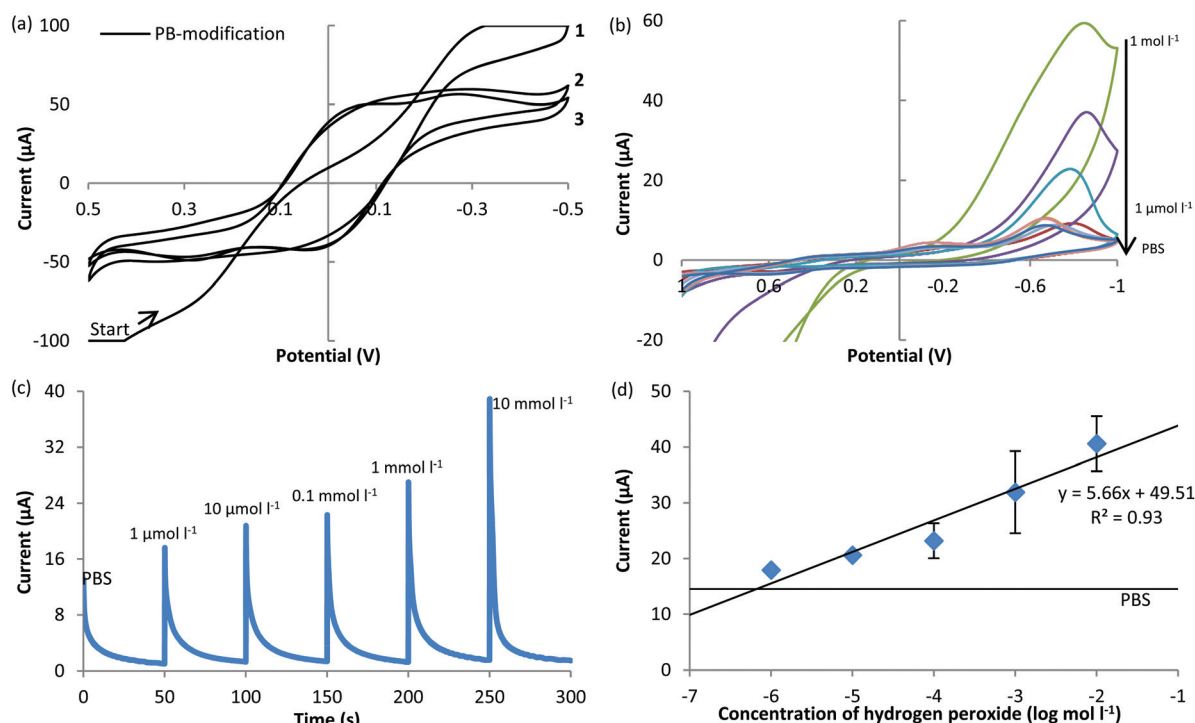


**Fig. 3** The characteristics of the PB-modified SP-IDME by using electrochemical measurement. (a) Cyclic voltammetry of PB modification. (b) CVs of different concentrations of  $\text{H}_2\text{O}_2$  when measured by using the PB-modified SP-IDME. (c) and (d) Amperometric measurement ( $i-t$ ) at  $-0.75$  V and the calibration curve when different concentrations of  $\text{H}_2\text{O}_2$  were tested.



PB film on the electrode surface based on the visual observation. Moreover, due to the electric connection of the SP-IDME, the working electrode and the reference electrode were connected to the same PB film, and the redox reaction of ferric ferrocyanide occurred simultaneously but individually on the two electrodes, doubling the redox potential reading ( $-0.75$  V in Fig. 3(b) compared to  $-0.36$  V vs. NHE). When the amperometric measurement at  $-0.75$  V was used to detect different concentrations of  $\text{H}_2\text{O}_2$  (Fig. 3(c)), the current decreased as the time increased, and the highest current response occurred at the beginning of the measurement. Considering that the sample stayed on the electrode surface during the measurement and no stirring was done to mix the sample, it appeared that the electrochemical reaction between PB and  $\text{H}_2\text{O}_2$  at the interface of the electrode and the media was diffusion limited. The PB-modified SP-IDME showed a linear relationship between the current peaks and the log concentration of  $\text{H}_2\text{O}_2$  in the range of  $1 \mu\text{mol l}^{-1}$  to  $10 \text{ mmol l}^{-1}$  (Fig. 3(d)), which could satisfy the requirement for the following tests.

#### Characterization of the synthesized ABs/ $\text{GOx}_{\text{ext}}$ /AuNPs/MBs- $\text{GOx}@$ PDA PMNCs

The synthesized ABs/ $\text{GOx}_{\text{ext}}$ /AuNPs/MBs- $\text{GOx}@$ PDA PMNCs in this study had two responsibilities: (1) recognition of the target bacteria, which requires the PMNCs to have the acceptable capability to isolate and concentrate the target bacteria from the sample media. (2) Conversion of the biological recognition to the electrochemical signal through the enzymatic reaction. The PMNCs which contained a large amount of GOx were expected to have high catalytic activity to induce a significant concentration change of glucose which could efficiently amplify the electrochemical signal. Therefore, tests to examine the binding affinity between the synthesized PMNCs and the target bacterial cells to obtain the electrochemical characteristics of the PMNCs were conducted at first.

The capture efficiency of using the synthesized PMNCs for *E. coli* O157:H7 at different concentrations is shown in Table 1. From the results, the PMNCs were able to capture approximately 89% or more of the target bacterial cells in the range of  $10^2$  to  $10^5 \text{ cfu ml}^{-1}$ . The rest, about 10% of the bacterial cells, was lost during the operation. The significant lower capture efficiency of PMNCs at  $10^1 \text{ cfu ml}^{-1}$  was probably due to the fact that the total number of bacterial cells in the sample is too small (maybe only one or two). The loss of an

individual cell in a small size group of cells was weighed much more than that in a large group of cells. Considering that there was an expected loss of bacterial cells due to the procedures like magnetic separation or pipetting, the capture efficiency of the PMNCs was acceptable, and the volume of PMNCs used in the test was followed throughout the study.

To verify the enzymatic activity of the synthesized PMNCs,  $20 \mu\text{l}$  of the ABs/ $\text{GOx}_{\text{ext}}$ /AuNPs/MBs- $\text{GOx}@$ PDA PMNCs were mixed with  $10 \text{ mmol l}^{-1}$  glucose solution and measured by CV at different time points during the glucose catalysis (Fig. 4). As shown in Fig. 4(a), there was a clear redox peak at about  $-0.4$  V and the current response at this redox peak potential increased when the reaction time was longer. The current responses at the redox peak were plotted against the enzymatic reaction time (Fig. 4(b)), showing that the enzyme activity reached the maximum rate at 5 min. This was used as the reaction time in the further test for the detection of *E. coli* O157:H7.

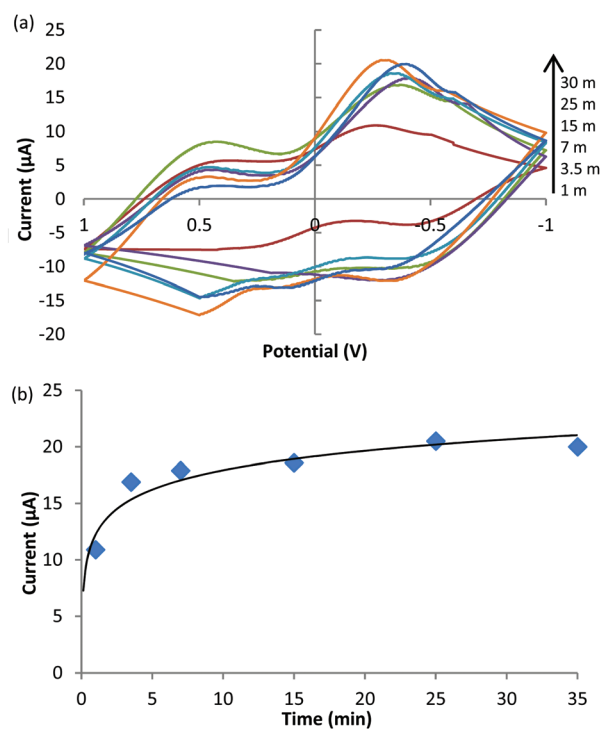


Fig. 4 Enzymatic activity of the synthesized PMNCs. (a) Cyclic voltammetry at different times of enzymatic reaction. (b) Redox peaks at different time points of the enzymatic reaction.

Table 1 Capture efficiencies of the synthesized ABs/ $\text{GOx}_{\text{ext}}$ /AuNPs/MBs- $\text{GOx}@$ PDA PMNCs for *E. coli* O157:H7

#	Volume of PMNCs ( $\mu\text{l}$ )	Volume of sample ( $\mu\text{l}$ )	Captured bacteria ( $\text{cfu ml}^{-1}$ )	Bacteria in waste ( $\text{cfu ml}^{-1}$ )	Capture efficiency (%)
1	20	200	$2 \times 10^1$	$1 \times 10^1$	66.7
2			$0.80 \pm 0.20 \times 10^2$	$0.05 \pm 0.05 \times 10^2$	94.1
3			$1.04 \pm 0.02 \times 10^3$	$0.12 \pm 0.00 \times 10^3$	89.6
4			$1.01 \pm 0.06 \times 10^4$	$0.12 \pm 0.00 \times 10^4$	89.4
5			$0.90 \pm 0.04 \times 10^5$	$0.11 \pm 0.01 \times 10^5$	89.1



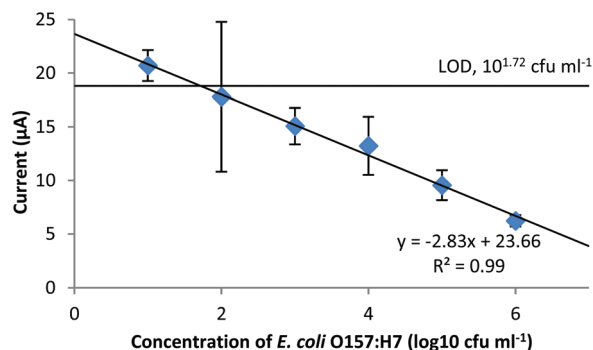


Fig. 5 Amperometric detection of *E. coli* O157:H7 in pure culture samples. The potential applied was  $-0.4$  V.

### The constructed electrochemical biosensor for the detection of *E. coli* O157:H7 in pure culture and the specificity of the biosensor

The amperometric detection (at  $-0.4$  V) of *E. coli* O157:H7 at different concentrations in the pure culture samples is shown in Fig. 5. From the figure, the current response is well-fitted into a simple linear regression against the concentration of

*E. coli* O157:H7 within the range of  $10^1$  to  $10^6$  cfu ml $^{-1}$  ( $R^2 = 0.99$ ). The obtained linear relationship between the current and the concentration of the bacteria has a negative slope, proving that more bacterial cells in the sample could retain more PMNCs at the filtration step and leave less PMNCs in the final glucose solution for the electrochemical measurement. The current response of negative control (NC) was  $25.83 \pm 2.34$   $\mu$ A. From the calibration curve, the limit of detection (LOD) of the constructed amperometric biosensor was  $10^{1.72}$  cfu ml $^{-1}$  (or 52 cfu ml $^{-1}$ ), which was determined by using the mean of the NC minus its standard deviation multiplied by three ( $S/N = 3$ ). The large deviation shown at  $10^2$  cfu ml $^{-1}$  was probably due to the small number of the bacterial cells present in the sample (approximately 20 cfu). At this concentration of the bacteria, a variation of several cells made a significant influence on the final results, where it is too weak to make a significant difference at lower concentrations ( $10^1$  cfu ml $^{-1}$ , or 1 cfu per sample) and not strong enough to reveal the differences at higher concentrations (more than  $10^3$  cfu ml $^{-1}$ ).

The LOD of the constructed amperometric biosensor was competitive to that of other electrochemical methods reported in previous publications (Table 2). On comparing the detection time, LODs, and strategies, our biosensor possesses several

Table 2 Comparison of the developed biosensors with other reported electrochemical methods for the detection of *E. coli* O157:H7

Electrochemical method	Detection			Range		Ref.
	Electrode	Strategy	Time	Culture	Food	
Amperometry	1st ABs/AuNPs-FeDC/SPCE	2nd AB-HRP	$\sim 30$ min	$5.75 \times 10^1$ to $5.75 \times 10^7$ cfu ml $^{-1}$ with an LOD of $6 \times 10^2$ cfu ml $^{-1}$	NA <sup>a</sup>	21
	Capture probe DNA/AuNPs/graphene oxide/GCE	Signal probe DNA/graphene oxide-thi-Au@SiO <sub>2</sub> /DNAzyme labeling	$\sim 1$ h 50 min	0.02 to 50.0 nmol l $^{-1}$ with an LOD of 0.01 nmol l $^{-1}$	NA	45
Electrochemical impedance spectroscopy	Platinum wire	Nanoporous alumina membrane-antibody	$\sim 2$ h	$10^2$ to $10^7$ cfu ml $^{-1}$ with an LOD of $10^2$ cfu ml $^{-1}$	NA	14
	Gold IDME	Magnetic NPs-AB-bacteria complex	$\sim 35$ min	$7.4 \times 10^4$ to $7.4 \times 10^7$ cfu ml $^{-1}$ with an LOD of $7.4 \times 10^4$ cfu ml $^{-1}$	$8.0 \times 10^5$ to $8.0 \times 10^7$ cfu ml $^{-1}$ with an LOD of $8.0 \times 10^5$ cfu ml $^{-1}$	17
	SEMs of DTSP on SP-IDME	Wheat germ agglutinin labeling	$\sim 45$ min without labeling $\sim 90$ min with labeling	$10^2$ to $10^6$ cfu ml $^{-1}$ with an LOD of $10^2$ cfu ml $^{-1}$ without WGA labeling	NA	18
	Reduced graphene oxide paper electrode	ABs/AuNPs/rGOPE direct detection	$\sim 30$ min	$1.5 \times 10^2$ to $1.5 \times 10^7$ cfu ml $^{-1}$ with an LOD of $1.5 \times 10^2$ cfu ml $^{-1}$	$1.5 \times 10^4$ cfu ml $^{-1}$ in ground beef, $1.5 \times 10^3$ cfu ml $^{-1}$ in cucumber	44
Cyclic voltammetry	Bio-AB/avidin/Au-SiO <sub>2</sub> /CHI-SH/Fc/C <sub>60</sub> /GCE	PtNCs-GOx-AB tag	$\sim 1$ h	$3.2 \times 10^1$ to $3.2 \times 10^6$ cfu ml $^{-1}$ with an LOD of 15 cfu ml $^{-1}$	NA	15
Amperometry	PB-modified SP-IDME	Bifunctional ABs/GOx <sub>ext</sub> /AuNPs/MBs-GOx@PDA PMNCs	$\sim 1$ h	$10^2$ to $10^6$ cfu ml $^{-1}$ with an LOD of 52 cfu ml $^{-1}$	$10^3$ to $10^6$ cfu g $^{-1}$ with an LOD of 190 cfu g $^{-1}$	This work

<sup>a</sup> NA: not available.



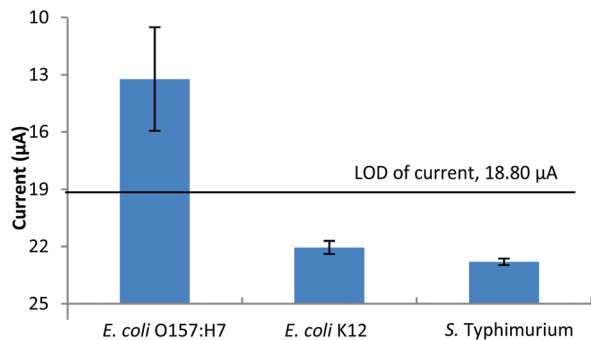


Fig. 6 Specificity of the constructed electrochemical biosensor for the detection of *E. coli* O157:H7.

merits such as it has a short detection time that is comparable to the electrochemical impedance sensors using a label-free strategy but yields an LOD that is similar to those obtained by the electrochemical sensors using labeling to amplify the signals. Based on the calculation of  $\text{LOD} \times \text{sample volume}$  (200  $\mu\text{l}$ ), the obtained LOD equals 10 cells. This is the result without any pre-enrichment. The generation time of *E. coli* under normal laboratory conditions is 15 to 20 min. Therefore, if the developed electrochemical biosensor could be combined with a pre-enrichment procedure, it would only require less than 2 h for a single cell to multiply and reach the detection limit. The detection procedure in this study was simple, only requiring the capture of the bacteria and a filtration step, which is beneficial if this biosensor is applied to on-site or in-field detection of the target bacteria.

The specificity of the constructed biosensor for the detection of *E. coli* O157:H7 is shown in Fig. 6. At  $10^4 \text{ cfu ml}^{-1}$ , the current response of the target bacteria had a difference of  $12.60 \mu\text{A}$  to that of the NC ( $25.83 \mu\text{A}$ ) which was significantly higher than that of *E. coli* K12 ( $3.77 \mu\text{A}$ ) and *S. typhimurium* ( $3.02 \mu\text{A}$ ). Moreover, neither the current responses of *E. coli* K12 nor *S. typhimurium* passed the LOD of current, which was  $18.80 \mu\text{A}$ . All of the above results suggest that the constructed biosensor was very specific for the detection of *E. coli* O157:H7. The specificity of the developed method was primarily determined by the polyclonal anti-*E. coli* antibody used. Based on the information of this antibody provided by the company, it reacts with many *E. coli* serotypes containing “O” and “K” antigens. The specificity of this method can be improved by using more specific antibodies if such a demand arises.

#### The validation of the constructed biosensor for the detection of *E. coli* O157:H7 in ground beef by using a handheld electrochemical detector

The validation for the detection of *E. coli* O157:H7 in ground beef using the established method and a handheld electrochemical detector to replace the benchtop electrochemical workstation was also conducted (Fig. 7). The current response of the NC was  $20.64 \pm 0.93 \mu\text{A}$ , which determined that the LOD of *E. coli* O157:H7 in ground beef was  $10^{2.28} \text{ cfu g}^{-1}$  ( $1.90 \times 10^2 \text{ cfu g}^{-1}$ ) using similar calculations as in the section “The con-

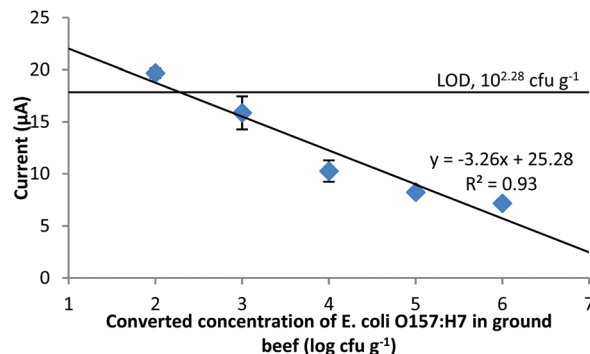


Fig. 7 The detection of *E. coli* O157:H7 in ground beef using a hand-held electrochemical detector.

structed electrochemical biosensor for the detection of *E. coli* O157:H7 in pure culture and the specificity of the biosensor”. This LOD is generally consistent with the result obtained from the pure culture if the ratio of the ground beef to the liquid sample (1 : 10 w/v) is taken into consideration. Comparing the current responses of different concentrations of *E. coli* O157:H7, the results from the food samples were slightly lower than those from the pure culture samples. The reason for this is probably that the complex food matrix contains various ingredients (fat, proteins, etc.) which could obstruct the free PMNCs from being separated from the supernatant, or adsorbed onto the free PMNCs and hindered them from passing through the filter. However, considering the fact that the final LOD of *E. coli* O157:H7 in ground beef was comparable to that in pure culture and the filtration step also helped in retaining food residues, which could reduce the noise, the results using the proposed electrochemical method are acceptable.

## Conclusion

In this study, we synthesized bifunctional ABs/ $\text{GOx}_{\text{ext}}$ /AuNPs/MBs- $\text{GOx}$ @PDA PMNCs, and fabricated an electrochemical biosensor coupled with a PB-modified SP-IDME for the rapid and sensitive detection of *E. coli* O157:H7 in pure culture and in food. The developed biosensor showed a broad detection range from  $10^2$  to  $10^6 \text{ cfu ml}^{-1}$  in the pure culture within 1 h. The validation of the developed approach to detect the target bacteria in ground beef demonstrated that it could detect as low as  $190 \text{ cfu g}^{-1}$  without a pre-enrichment procedure, and the possibility of using a handheld device to achieve the electrochemical measurement which demonstrates the benefit for on-site or in-field applications by using the proposed method. To conclude, the developed electrochemical biosensor requires a short detection time similar to that of the sensors using a label-free strategy but also with efficient amplification to achieve low LOD which is comparable to others using various labeling strategies. The advantages of using bifunctional PMNCs in this study exhibited a new direction to



construct electrochemical biosensors for sensitive and rapid detection of foodborne pathogens.

## Acknowledgements

This research was supported in part by ABI (project # 0380-43052-24-2333) and Aibit (project # 30-011905). The authors want to thank Dr David W. Paul and Zach Callaway for their help in revising the manuscript, and also thank Lisa Kelso for her help in microbial tests.

## References

- 1 CDC (Centers for Disease Control and Prevention), *E. coli* (*Escherichia coli*). <http://www.cdc.gov/ecoli/general/index.html#what-are-shiga-toxin>, (last updated November 2015).
- 2 P. M. Griffin and R. V. Tauxe, *Epidemiol. Rev.*, 1991, **13**, 60–98.
- 3 N. L. Padola, *Front. Microbiol.*, 2014, **5**, 1–2.
- 4 S. Hoffmann and T. D. Anekwe, EIB-118, USDA, U.S. Department of Agriculture, Economic Research Service, 2013.
- 5 CDC (Centers for Disease Control and Prevention), *Multi-state outbreak of Shiga toxin-producing Escherichia coli O157 infections linked to Costco rotisserie chicken salad*. <http://www.cdc.gov/ecoli/2015/o157h7-11-15/index.html> (last updated 3.2.2016).
- 6 CDC (Centers for Disease Control and Prevention), *Multi-state outbreak of Shiga toxin-producing Escherichia coli O157 infections linked to alfalfa sprouts produced by Jack & the Green Sprouts*. <http://www.cdc.gov/ecoli/2016/o157-02-16/index.html> (last updated 12.22.2015).
- 7 Z. Fu, S. Rogelj and T. L. Kieft, *J. Food Microbiol.*, 2005, **99**, 47–57.
- 8 H. P. Dwivedi and L.-A. Jaykus, *Crit. Rev. Microbiol.*, 2011, **37**, 40–63.
- 9 K. J. Yoshitomi, K. C. Jinneman, R. Zapata, S. D. Weagant and W. M. Fedio, *J. Food Sci.*, 2012, **77**, 481–489.
- 10 I. Palchetti and M. Mascini, *Anal. Bioanal. Chem.*, 2008, **391**, 455–471.
- 11 J. Monzo, I. Insua, F. Fernandez-Trillo and P. Rodriguez, *Analyst*, 2015, **140**, 7116–7128.
- 12 A. J. Bard and L. R. Faulkner, *Electrochemical methods. Fundamentals and Applications*, John Wiley & Sons Inc., New York, 2nd edn, 2001.
- 13 C.-K. Joung, H.-N. Kim, M.-C. Lim, T.-J. Jeon, H.-Y. Kim and Y.-R. Kim, *Biosens. Bioelectron.*, 2013, **44**, 210–215.
- 14 F. Tan, P. H. M. Leung, Z.-B. Liu, Y. Zhang, L. Xiao, W. Ye, X. Zhang, L. Yi and M. Yang, *Sens. Actuators, B*, 2011, **159**, 328–335.
- 15 Y. Li, L. Fang, P. Cheng, J. Deng, L. Jiang, H. Huang and J. Zheng, *Biosens. Bioelectron.*, 2013, **49**, 485–491.
- 16 E. I. Maurer, K. K. Comfort, S. M. Hussain, J. J. Schlager and S. M. Mukhopadhyay, *Sens.*, 2012, **21**, 8135–8144.
- 17 M. Varshney, Y. Li, B. Srinivasan and S. Tung, *Sens. Actuators, B*, 2007, **128**, 99–107.
- 18 Z. Li, Y. Fu, W. Fang and Y. Li, *Sens.*, 2015, **15**, 19212–19224.
- 19 M. Xu, R. Wang and Y. Li, *Talanta*, 2016, **148**, 200–208.
- 20 E. B. Settingington and E. C. Alocilja, *Biosensors*, 2012, **2**, 15–31.
- 21 Y.-H. Lin, S.-H. Chen, Y.-C. Chuang, Y.-C. Lu, T. Y. Shen, C. A. Chang and C.-S. Lin, *Biosens. Bioelectron.*, 2008, **23**, 1832–1837.
- 22 S. Chemburu, E. Wilkins and I. Abdel-Hamid, *Biosens. Bioelectron.*, 2005, **21**, 491–499.
- 23 G. A. Zelada-Guillen, S. V. Bhosale, J. Riu and F. X. Rius, *Anal. Chem.*, 2010, **82**, 9254–9260.
- 24 M. Varshney and Y. Li, *Biosens. Bioelectron.*, 2007, **22**, 2408–2414.
- 25 A. Shabani, M. Zourob, B. Allain, C. A. Marquette, M. F. Lawrence and R. Mandeville, *Anal. Chem.*, 2008, **80**, 9475–9482.
- 26 H. Lee, S. M. Dellatore, W. M. Miller and P. B. Messersmith, *Sci.*, 2007, **318**, 426–430.
- 27 X. Liu, J. Cao, H. Li, J. Li, Q. Jin, K. Ren and J. Ji, *ACS Nano*, 2013, **7**, 9384–9395.
- 28 Q. Wei, F. Zhang, J. Li, B. Li and C. Zhao, *Polym. Chem.*, 2010, **1**, 1430–1433.
- 29 C.-C. Ho and S.-J. Ding, *J. Biomed. Nanotechnol.*, 2014, **10**, 3063–3084.
- 30 V. Ball, D. del Frari, V. Toniazio and D. Ruch, *J. Colloid Interface Sci.*, 2012, **386**, 366–372.
- 31 X. Gu, Y. Zhang, H. Sun, X. Song, C. Fu and P. Dong, *J. Nanomater.*, 2014, **2015**, 1–12.
- 32 D. R. Dreyer, D. J. Miller, B. D. Freeman, D. R. Paul and C. W. Bielawski, *Chem. Sci.*, 2013, **4**, 3796–3802.
- 33 D. A. Kanayeva, R. Wang, D. Rhoads, G. F. Erf, M. K. Slavik, S. Tung and Y. Li, *J. Food Prot.*, 2012, **75**, 1951–1959.
- 34 Y. Fu, P. Li, L. Bu, T. Wang, Q. Xie, X. Xu, L. Lei, C. Zou and S. Yao, *J. Phys. Chem. C*, 2010, **114**, 1472–1480.
- 35 J. Zhang, S. Song, L. Wang, D. Pan and C. Fan, *Nat. Protoc.*, 2007, **2**, 2888–2897.
- 36 Y. Lin, L. Hu, L. Yin and L. Guo, *Sens. Actuators, B*, 2015, **210**, 513–518.
- 37 L. C. Clark and C. Lyons, *Ann. N. Y. Acad. Sci.*, 1962, **102**, 29–45.
- 38 A. A. Karyakin, O. V. Gitelmacher and E. E. Karyakina, *Anal. Chem.*, 1995, **67**, 2419–2423.
- 39 W.-Z. Jia, K. Wang and X.-H. Xia, *Trends Anal. Chem.*, 2010, **29**, 306–318.
- 40 M. M. Rahman, A. J. S. Ahammad, J.-H. Jin, S. J. Ahn and J.-J. Lee, *Sens.*, 2010, **10**, 4855–4886.
- 41 E.-H. Yoo and S.-Y. Lee, *Sens.*, 2010, **10**, 4558–4576.
- 42 A. L. Galant, R. C. Kaufman and J. D. Wilson, *Food Chem.*, 2015, **188**, 149–160.
- 43 X. Ji, J. Ren, R. Ni and X. Liu, *Analyst*, 2010, **135**, 2092–2098.
- 44 Y. Wang, J. Ping, Z. Ye, J. Wu and Y. Ying, *Biosens. Bioelectron.*, 2013, **49**, 492–498.
- 45 Y. Li, J. Deng, L. Fang, K. Yu, H. Huang, L. Jiang, W. Liang and J. Zheng, *Biosens. Bioelectron.*, 2015, **63**, 1–6.

